Electronic Supplementary Material (ESI) for Journal of Materials Chemistry C.

SUPPORTING INFORMATION

Synergetic Effect-triggered Performance Promotion in $Sr_{3-x}Ba_xP_5N_{10}Cl:Eu^{2+}$ Phosphors

Hsi-Ping Hsueh,[‡a] Mu-Huai Fang,[‡a] Thangaraji Vasudevan,[a] Wen-Tse Huang,[a] Natalia Majewska,[b] Agata Lazarowska,[b] Sebastian Mahlik,[b,*] Hwo-Shuenn Sheu,[c] Jyh-Fu Lee,[c] and Ru-Shi Liu[a,*]

[a]Department of Chemistry, National Taiwan University, Taipei 106, Taiwan

[b]Institute of Experimental Physics, Faculty of Mathematics, Physics and Informatics, University of Gdańsk, Wita Stwosza 57, 80-308 Gdańsk, Poland

[c]National Synchrotron Radiation Research Center, Hsinchu 300, Taiwan

EXPERIMENTAL METHODS

Reagents. Barium nitride (Ba_3N_2; 99.7%), strontium nitride (Sr_3N_2; 99.5%), Barium chloride ($BaCl_2$; 99.0%), Strontium chloride ($SrCl_2$; 99.0%) and europium nitride (EuN; 99.9%) were obtained from Materion. Phosphorus red (P_{red}, 98.9%) was purchased from Acros organics.

Synthesis of $Sr_{2.91-x}Ba_xP_5N_{10}Cl:0.09Eu^{2+}$. All experiments were conducted in an inert gas-filled glovebox (O_2 < 1 ppm, H_2O < 1 ppm) due to the moisture sensitivity of the starting materials. The starting materials were mixed in an agate mortar and placed in tungsten crucibles in a hot isostatic press (HIP; AIP6-30H, American Isostatic Presses, Inc., Columbus, OH, USA). The samples were heated to 1000 °C at a rate of 20 °C/min under 150 MPa pressure, and the conditions were maintained for 10 h. The samples were cooled to room temperature (RT), and $Sr_{2.91-x}Ba_xP_5N_{10}Cl:0.09Eu^{2+}$ phosphors were obtained.

Characterization. The as-prepared powder samples were examined by X-ray diffraction (XRD) analysis using a D2 PHASER diffractometer (Bruker) with CuKα radiation source (λ = 1.5418 Å). Synchrotron powder X-ray diffraction patterns of $Sr_{2.91-x}Ba_xP_5N_{10}Cl:0.09Eu^{2+}$ were acquired using 15keV X-ray (λ = 0.82657Å) from the National Synchrotron Radiation Research Center (Taiwan) BL01C2 beamline at room temperature (RT) by using a Debye–Scherrer camera. The pattern was used for Rietveld analysis using Total Pattern Analysis Solutions software (TOPAS 4.2). Data on particle size were collected using the Multisizer 3 (Beckman Coulter) particle size analyzer. The morphologies of the as-prepared samples were observed using scanning electron microscopy (SEM, JSM-6510, JEOL) at Advanced Research Center for Green Materials Science and Technology (ARC-GMST), National Taiwan University, Taipei City, Taiwan. RT photoluminescence (PL) and photoluminescence excitation (PLE) spectra were measured with a FluoroMax-4P spectrofluorometer (Horiba) equipped with a 150 W xenon lamp as an excitation source and an R928 Hamamatsu photomultiplier as a detector to record the PL and PLE spectra within the spectral range of 250–850 nm. The internal quantum efficiency (IQE) was measured with a Hamamatsu absolute PL quantum yield spectrometer C11347. PL spectra were obtained with an Andor SR-750-D1 spectrometer equipped with a CCD camera (DU420A-OE). A Kimmon Koha He-Cd laser (442 nm) was used as an excitation source. Decay profiles were obtained using time-resolved spectroscopy apparatus equipped with a PG 401/SH optical parametric generator pumped by a PL2251A pulsed YAG:Nd laser (EKSPLA). The detection part consisted of a 2501S grating spectrometer (Bruker Optics) combined with a C4334-01 streak camera (Hamamatsu). Data were recorded in the form of streak images on a 640 × 480 pixel CCD array. Photon-counting algorithm–based software was used to transform the result into a 2D matrix of photon

counts versus wavelength and time (streak image). X-ray absorption spectroscopy was measured at the BL17C1 beamline of the National Taiwan Synchrotron Radiation Research Center (NSRRC), Hsinchu City, Taiwan. Data analysis was conducted using Athena software

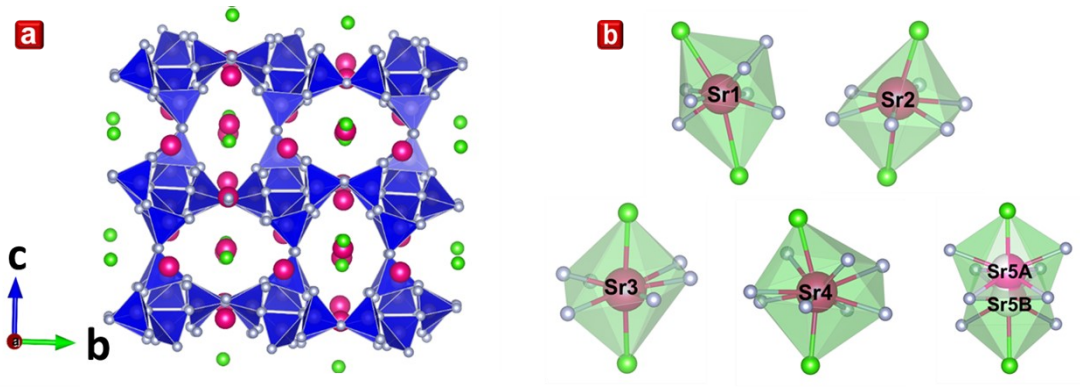

Figure S1. (a) Crystal structure of $Sr_{2.91-x}Ba_xP_5N_{10}Cl{:}0.09Eu^{2+}$ (x = 0, 1, 2, and 2.91). Green atoms represent Cl^- ions, magenta atoms represent Sr^{2+} ions, and blue tetrahedra represent P^{5+} ions surrounded by four N^{3-} ions. (b) Coordinated environment of Sr1, Sr2, Sr3, Sr4, and Sr5 sites.

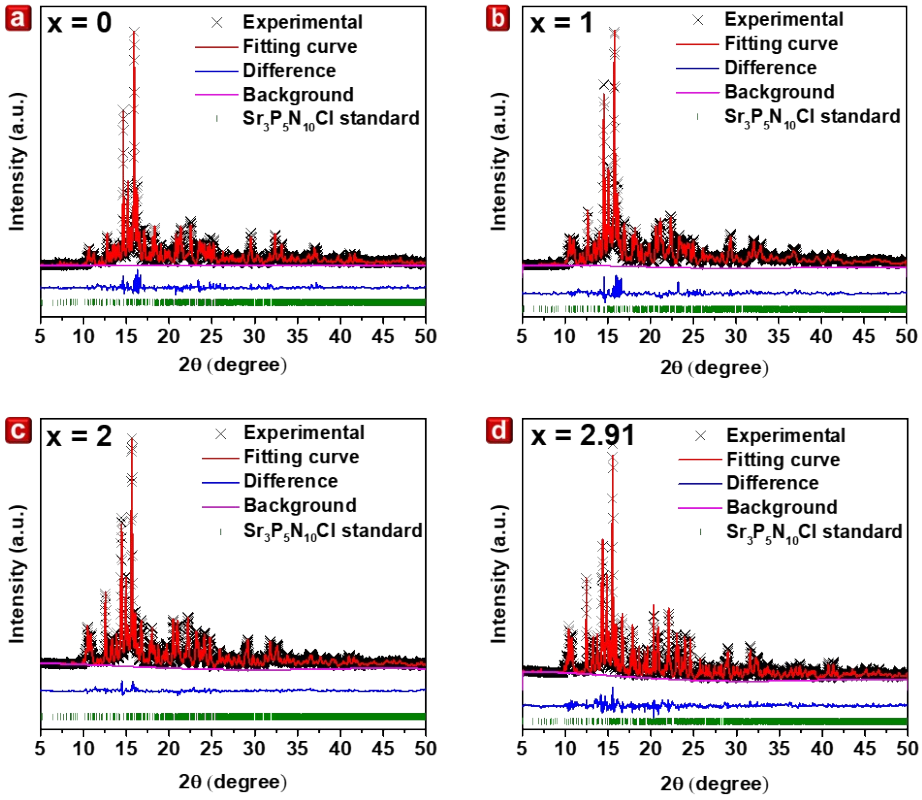

Figure S2. Rietveld refinement patterns of the crystal structure of

$Sr_{2.91-x}Ba_xP_5N_{10}Cl:0.09Eu^{2+}$. (a) x = 0, (b) x = 1, (c) x = 2, and (d) x = 2.91.

Table S1. Atomic positions derived from the Rietveld refinement of $Sr_{2.91-x}Ba_xP_5N_{10}Cl:0.09Eu^{2+}$ (x = 0).

Site	x	y	z	Atom	Occ	Beq (Å^2)
Sr1	0.28251(34)	0.01610(37)	0.32288(34)	Sr	1	2.66(13)
Sr2	0.04219(55)	0.25	0.73367(55)	Sr	1	3.15(21)
Sr3	0.04537(44)	0.25	0.24201(47)	Sr	1	0.17(16)
Sr4	0.33455(55)	0.25	0.02161(55)	Sr	1	2.77(22)
Sr5A	0.33541(85)	0.25	0.58969(78)	Sr	0.6534(68)	1.95(26)
Sr5B	0.3391(13)	0.25	0.4864(15)	Sr	0.3466(68)	0.03(39)
Cl1	0.2762(12)	0.25	0.8037(10)	Cl	1	0.66(35)
Cl2	0.2998(10)	0.25	0.2562(10)	Cl	1	0.99(32)
P1	0.0261(10)	0.0249(12)	0.63319(92)	P	1	3.52(41)
P2	0.03436(90)	0.5343(11)	0.15044(87)	P	1	2.33(33)
P3	0.0806(11)	0.13087(97)	0.02477(90)	P	1	1.72(34)
P4	0.0847(11)	0.13433(96)	0.46816(94)	P	1	1.37(32)
P5	0.2448(12)	0.5116(11)	0.07314(77)	P	1	2.23(28)
N1	0.0114(24)	0.0931(24)	0.1060(22)	N	1	0.70(85)
N2	0.0094(25)	0.1159(24)	0.5664(24)	N	1	0.02(83)
N3	0.0221(20)	0.0545(16)	0.7571(28)	N	1	0.02(60)
N4	0.0798(23)	0.0699(21)	0.3665(21)	N	1	0.02(72)
N5	0.1861(18)	0.5248(21)	0.1873(19)	N	1	0.02(69)
N6	0.2963(29)	0.5918(30)	0.5047(26)	N	1	2.22(79)
N7	0.2259(30)	0.0987(32)	0.5093(31)	N	1	4.4(11)
N8	0.3541(21)	0.0375(24)	0.1291(22)	N	1	0.02(73)
N9	0.0094(22)	0.6248(24)	0.0903(22)	N	1	0.02(82)
N10	0.0872(33)	0.25	0.0612(29)	N	1	0.02(10)
N11	0.0926(39)	0.25	0.4358(41)	N	1	3.8(15)

Table S2. Atomic positions derived from the Rietveld refinement of $Sr_{2.91-x}Ba_xP_5N_{10}Cl:0.09Eu^{2+}$ (x = 1).

Site	x	y	z	Atom	Occ	Beq (Å^2)
Sr1	0.27983(33)	0.01548(37)	0.32344(30)	Sr	0.70(47)	2.59(13)
Ba1	0.27983(33)	0.01548(37)	0.32344(30)	Ba	0.30(47)	2.59(13)
Sr2	0.04144(57)	0.25	0.73431(53)	Sr	0.672(17)	3.45(23)
Ba2	0.04144(57)	0.25	0.73431(53)	Ba	0.328(17)	3.45(23)
Sr3	0.04226(47)	0.25	0.24392(44)	Sr	0.662(16)	0.06(16)
Ba3	0.04226(47)	0.25	0.24392(44)	Ba	0.338(16)	0.06(16)
Sr4	0.33551(45)	0.25	0.02151(45)	Sr	0.530(14)	0.66(17)
Ba4	0.33551(45)	0.25	0.02151(45)	Ba	0.470(14)	0.66(17)
Sr5A	0.33654(95)	0.25	0.59318(83)	Sr	0.37(66)	1.52(31)
Ba5A	0.33654(95)	0.25	0.59318(83)	Ba	0.16(41)	1.52(31)
Sr5B	0.3393(12)	0.25	0.5093(14)	Sr	0.38(67)	2.60(41)
Ba5B	0.3393(12)	0.25	0.5093(14)	Ba	0.1(10)	2.60(41)
Cl1	0.2685(13)	0.25	0.7957(11)	Cl	1	0.20(40)
Cl2	0.2996(12)	0.25	0.2667(12)	Cl	1	1.93(41)
P1	0.0314(11)	0.0231(12)	0.63835(97)	P	1	1.52(39)
P2	0.0415(10)	0.5266(13)	0.1531(10)	P	1	3.56(41)
P3	0.0801(10)	0.13091(99)	0.02032(91)	P	1	0.04(33)
P4	0.0872(13)	0.1312(12)	0.4690(11)	P	1	3.19(40)
P5	0.2423(14)	0.5149(12)	0.07579(80)	P	1	0.70(27)
N1	0.9887(25)	0.0843(26)	0.1000(26)	N	1	0.02(90)
N2	0.0122(27)	0.1147(25)	0.5563(30)	N	1	0.02(88)
N3	0.0288(22)	0.0528(18)	0.7597(29)	N	1	0.02(68)
N4	0.0770(28)	0.0755(22)	0.3606(23)	N	1	0.02(80)
N5	0.1753(19)	0.5278(25)	0.1824(21)	N	1	0.02(79)
N6	0.3051(28)	0.5921(26)	0.5068(30)	N	1	0.76(80)
N7	0.2279(28)	0.0976(26)	0.4884(32)	N	1	1.7(10)
N8	0.3541(26)	0.0300(26)	0.1190(26)	N	1	0.02(82)
N9	0.0004(25)	0.6207(28)	0.0795(25)	N	1	1.7(11)
N10	0.0989(36)	0.25	0.0557(33)	N	1	1.2(13)
N11	0.0860(45)	0.25	0.4208(44)	N	1	7.0(19)

Table S3. Atomic positions derived from the Rietveld refinement of $Sr_{2.91-x}Ba_xP_5N_{10}Cl{:}0.09Eu^{2+}$ (x = 2).

Site	x	y	z	Atom	Occ	Beq (Å^2)
Sr1	0.27412(20)	0.01051(25)	0.32368(16)	Sr	0.36(34)	1.7(98)
Ba1	0.27412(20)	0.01051(25)	0.32368(16)	Ba	0.64(34)	1.6(33)
Sr2	0.03726(36)	0.25	0.73485(33)	Sr	0.345(15)	3(11)
Ba2	0.03726(36)	0.25	0.73485(33)	Ba	0.655(15)	2.2(32)
Sr3	0.04245(30)	0.25	0.24273(29)	Sr	0.269(15)	1(11)
Ba3	0.04245(30)	0.25	0.24273(29)	Ba	0.731(15)	0.6(23)
Sr4	0.33801(31)	0.25	0.02381(34)	Sr	0.178(13)	2(13)
Ba4	0.33801(31)	0.25	0.02381(34)	Ba	0.822(13)	1.3(16)
Sr5A	0.33264(63)	0.25	0.57419(54)	Sr	0.23(48)	1(19)
Ba5A	0.33264(63)	0.25	0.57419(54)	Ba	0.31(30)	0.8(83)
Sr5B	0.33815(75)	0.25	0.51648(83)	Sr	0.26(48)	0.7063
Ba5B	0.33815(75)	0.25	0.51648(83)	Ba	0.20(74)	0.7063
Cl1	0.2703(10)	0.25	0.79274(95)	Cl	1	1.22(33)
Cl2	0.3015(10)	0.25	0.28079(98)	Cl	1	2.51(36)
P1	0.03080(86)	0.0174(10)	0.63539(78)	P	1	2.93(33)
P2	0.03965(80)	0.52713(93)	0.15275(78)	P	1	2.44(27)
P3	0.07769(75)	0.13671(69)	0.02045(69)	P	1	0.25(23)
P4	0.08535(92)	0.13090(81)	0.47328(86)	P	1	2.50(28)
P5	0.24409(94)	0.51485(80)	0.07932(52)	P	1	0.44(19)
N1	0.0162(21)	0.0889(21)	0.0980(20)	N	1	0.72(73)
N2	0.0095(20)	0.1135(20)	0.5564(21)	N	1	0.02(66)
N3	0.0178(18)	0.0598(13)	0.7580(23)	N	1	0.02(53)
N4	0.0801(21)	0.0743(19)	0.3657(18)	N	1	0.02(62)
N5	0.1759(17)	0.5421(19)	0.1668(18)	N	1	0.61(65)
N6	0.3238(18)	0.5763(17)	0.4943(20)	N	1	0.02(60)
N7	0.2327(20)	0.0988(17)	0.5076(24)	N	1	1.39(67)
N8	0.3593(20)	0.0308(21)	0.1173(18)	N	1	0.02(62)
N9	0.0000(20)	0.6165(21)	0.0796(20)	N	1	0.02(70)
N10	0.1191(30)	0.25	0.0466(29)	N	1	3.2(11)
N11	0.0727(23)	0.25	0.4606(26)	N	1	0.02(93)

Table S4. Atomic positions derived from the Rietveld refinement of $Sr_{2.91-x}Ba_xP_5N_{10}Cl{:}0.09Eu^{2+}$ (x = 2.91).

Site	x	y	z	Atom	Occ	Beq (Å^2)
Ba1	0.26437(43)	0.00456(58)	0.32289(25)	Ba	1	2.42(12)
Ba2	0.03703(82)	0.25	0.73409(82)	Ba	1	3.55(27)
Ba3	0.03664(68)	0.25	0.23718(68)	Ba	1	0.47(20)
Ba4	0.33775(79)	0.25	0.02874(85)	Ba	1	1.33(23)
Ba5A	0.3339(13)	0.25	0.54592(97)	Ba	0.697(14)	2.80(37)
Ba5B	0.3524(22)	0.25	0.5201(23)	Ba	0.303(14)	0.01(58)
Cl1	0.2732(23)	0.25	0.7864(24)	Cl	1	1.12(66)
Cl2	0.2953(19)	0.25	0.2896(22)	Cl	1	0.01(56)
P1	0.0311(21)	0.0317(20)	0.6376(20)	P	1	5.03(74)
P2	0.0361(18)	0.5243(18)	0.1442(17)	P	1	1.34(45)
P3	0.0861(18)	0.1427(14)	0.0051(15)	P	1	0.06(41)
P4	0.0831(23)	0.1190(19)	0.4828(21)	P	1	5.96(73)
P5	0.2552(27)	0.4944(24)	0.07250(91)	P	1	0.47(29)
N1	0.0029(40)	0.0869(48)	0.0878(41)	N	1	1.1(17)
N2	0.0319(49)	0.0951(45)	0.5758(42)	N	1	0.01(14)
N3	0.0077(34)	0.0357(25)	0.7393(41)	N	1	0.01(11)
N4	0.0553(48)	0.0888(41)	0.3959(41)	N	1	2.1(13)
N5	0.1352(38)	0.5492(41)	0.1511(36)	N	1	0.3(13)
N6	0.2886(65)	0.5970(66)	0.5086(69)	N	1	1.8(19)
N7	0.2099(58)	0.0995(63)	0.5061(60)	N	1	0.01(18)
N8	0.3359(40)	0.0323(39)	0.1204(35)	N	1	0.01(12)
N9	0.0000(33)	0.6108(39)	0.1030(36)	N	1	0.01(12)
N10	0.0822(51)	0.25	0.0560(47)	N	1	0.01(16)
N11	0.0714(53)	0.25	0.4705(58)	N	1	1.3(18)

Table S5. Lattice parameters derived from the Rietveld refinement of $Sr_{2.91-x}Ba_xP_5N_{10}Cl{:}0.09Eu^{2+}$ (x = 0, 1, 2, and 2.91).

	x = 0	x = 1	x = 2	x = 2.91
Crystal system	Orthorhombic			
Space group	*Pnma*			
R_{wp}	7.17%	5.92%	3.93%	6.43%
R_p	5.23%	4.11%	2.84%	4.75%
χ^2	2.31	2.20	1.46	2.36

	x = 0	x = 1	x = 2	x = 2.91
a	12.24386(68) Å	12.3560(11) Å	12.45928(51) Å	12.53678(58) Å
b	12.95688(70) Å	13.0349(11) Å	13.11802(49) Å	13.19606(55) Å
c	13.43521(84) Å	13.5376(14) Å	13.67301(63) Å	13.79622(63) Å
V	2131.39(21) Å^3	2180.36(35) Å^3	2234.73(16) Å^3	2282.39(18) Å^3

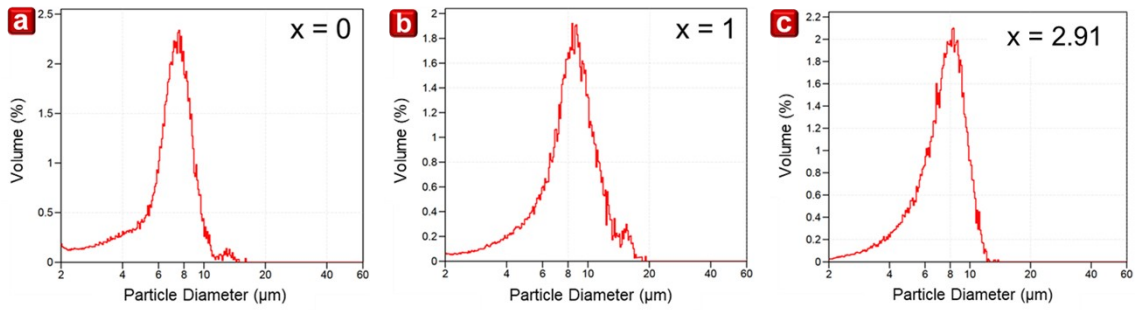

Figure S3. Particle size distribution of $Sr_{2.91-x}Ba_xP_5N_{10}Cl:0.09Eu^{2+}$. (a) $x = 0$, (b) $x = 1$, and (c) $x = 2.91$.

Table S6. Particle size from the Coulter analyzer of $Sr_{2.91-x}Ba_xP_5N_{10}Cl:0.09Eu^{2+}$ ($x = 0$, 1, 2, and 2.91).

Sample	Average Particle Size (μm)	d_{10} (μm)	d_{50} (μm)	d_{90} (μm)	$(d_{90}-d_{10})/d_{50}$
x = 0	6.843	3.852	7.069	9.001	0.73
x = 1	8.319	4.773	8.290	11.600	0.82
x = 2	8.138	5.477	8.340	10.390	0.59
x = 2.91	7.343	4.625	7.528	9.704	0.67

d_{10}: 10% of the particle size smaller than this value.
d_{50}: 50% of the particle size smaller and larger this value, also known as the median particle size.
d_{90}: 90% of the particle size smaller than this value.
Equation of $(d_{90} - d_{10})/d_{50}$ could be used to identify the particle size distribution.

Table S7. Internal quantum efficiency excited by 420 nm for $Sr_{2.91-x}Ba_xP_5N_{10}Cl:0.09Eu^{2+}$ ($x = 0$, 1, 2, and 2.91).

Samples	Internal Quantum Efficiency (%)
x = 0	21.8
x = 1	35.6
x = 2	37.0
x = 2.91	11.4

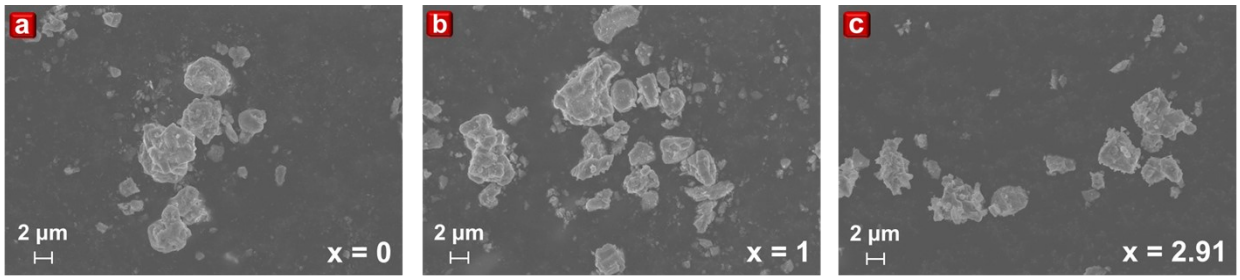

Figure S4. SEM Images of $Sr_{2.91-x}Ba_xP_5N_{10}Cl$:0.09$Eu^{2+}$. (a) x = 0, (b) x = 1, and (c) x =2.91.

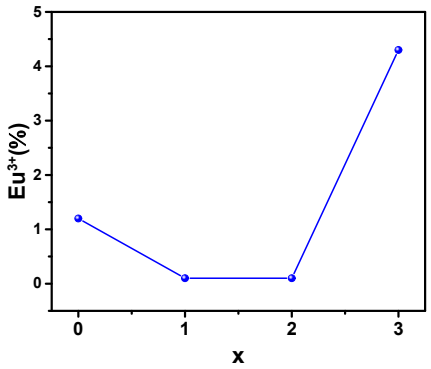

Figure S5. Eu^{3+} ratio from curve fitting for $Sr_{2.91-x}Ba_xP_5N_{10}Cl$:0.09$Eu^{2+}$ (x = 0, 1, 2, and 2.91).

Table S8. Eu^{2+} and Eu^{3+} ratio from curve fitting for $Sr_{2.91-x}Ba_xP_5N_{10}Cl$:0.09$Eu^{2+}$ (x = 0, 1, 2, and 2.91).

Sample	Eu^{2+}(%)	Eu^{3+}(%)
x = 0	98.8	1.2
x = 1	99.9	0.1
x = 2	99.9	0.1
x = 2.91	95.7	4.3

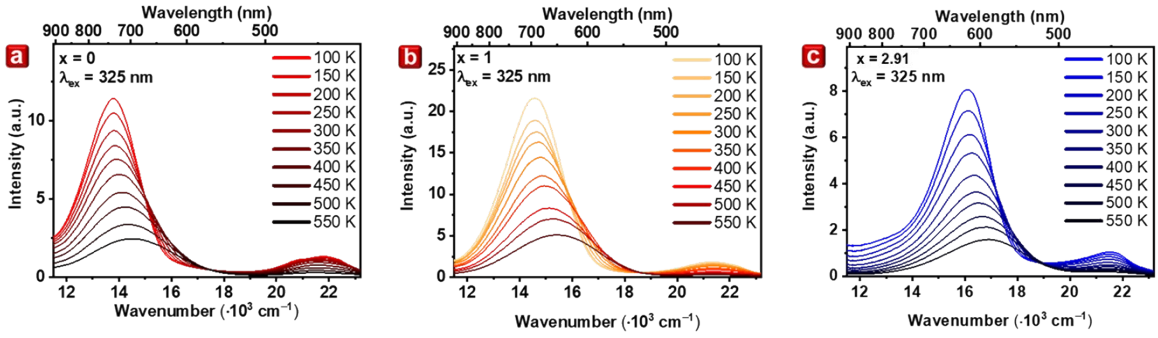

Figure S6. Temperature-dependent PL upon excitation at 325 nm and temperature range 100–550 K of $Sr_{2.91-x}Ba_xP_5N_{10}Cl:0.09Eu^{2+}$. (a) x = 0, (b) x = 1, and (c) x = 2.91.

Table S9. Activation energy parameters E_A and probability of nonradiative transition p_{nr} for Eu2 emission for $Sr_{2.91-x}Ba_xP_5N_{10}Cl:0.09Eu^{2+}$($x$ = 0, 1, 2, and 2.91).

Sample	E_A (cm^{-1})	p_{nr} ($\cdot 10^6$ s^{-1})
x = 0	1210 ± 150	3.7
x = 1	1064 ± 110	4.5
x = 2	1057 ± 40	5.2
x = 2.91	600 ± 40	3.1

Table S10. Huang–Rhys factor S, effective phonon energy $\hbar\omega$, and energy of electron lattice relaxation $S\hbar\omega$ parameters calculated from equation (2).

Sample	S	$\hbar\omega$ (cm^{-1})	$S\hbar\omega$ (cm^{-1})
x = 0	9	342±1	3078±9
x = 1	9	365±2	3285±18
x = 2	9	368±7	3312±63
x = 2.91	9	349±2	3141±18

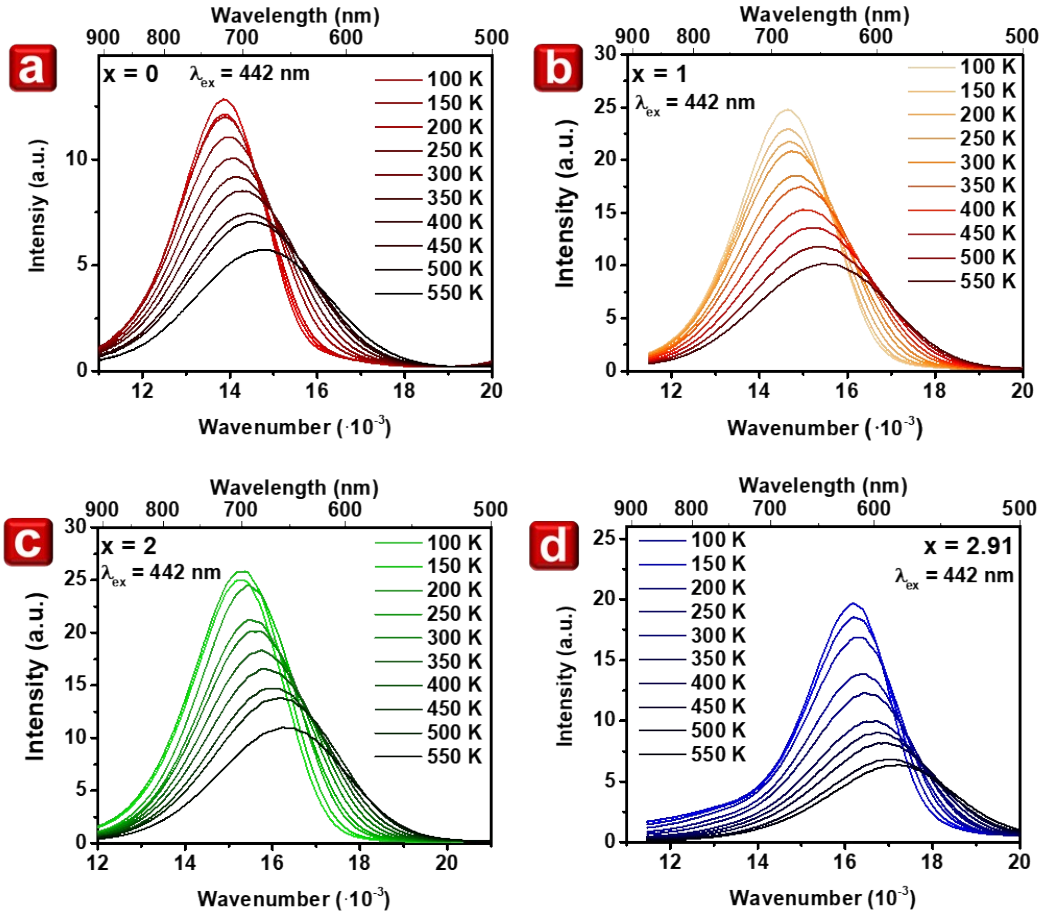

Figure S7. Temperature-dependent PL upon excitation at 442 nm and temperature range 100–550 K of $Sr_{2.91-x}Ba_xP_5N_{10}Cl$:0.09$Eu^{2+}$. (a) x = 0, (b) x = 1, (c) x = 2, and (d) x = 2.91.

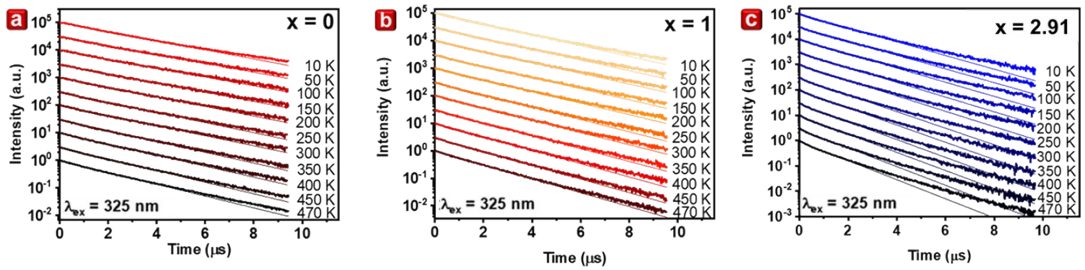

Figure S8. Temperature-dependent decay profiles for Eu2 of $Sr_{2.91-x}Ba_xP_5N_{10}Cl$:0.09$Eu^{2+}$. (a) x = 0, (b) x = 1, and (c) x = 2.91.

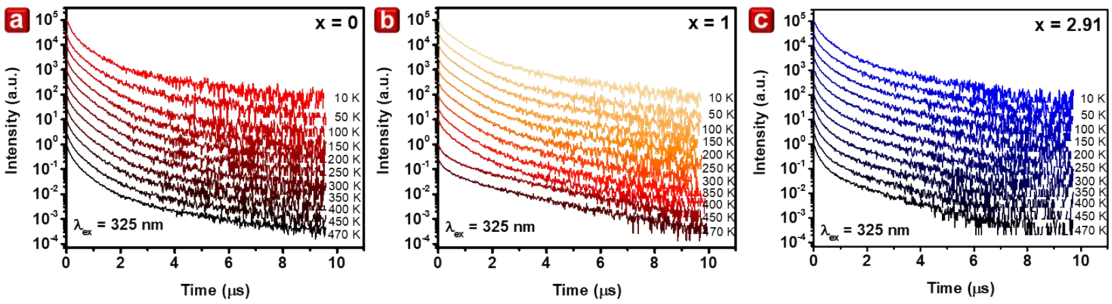

Figure S9. Temperature-dependent decay profiles for Eu1 of $Sr_{2.91-x}Ba_xP_5N_{10}Cl:0.09Eu^{2+}$. (a) x = 0, (b) x = 1, and (c) x = 2.91.